Causal Reduced-Order Modeling of Distributed Structures in a Transient Circuit Simulator

Ramya Mohan, Myoung J. Choi, Stephen E. Mick, Frank P. Hart, Karthik Chandrasekar, Andreas C. Cangellaris, *Fellow*, *IEEE*, Paul D. Franzon, *Senior Member*, *IEEE* and Michael B. Steer, *Fellow*, *IEEE*

***Abstract*— Fosters' canonical representation of the transfer characteristic of a linear system is the key to causal, fully convergent, incorporation of distributed structures in transient circuit simulators. The implementation of the Foster's model in the fREEDA® circuit simulator is reported and the modeling of a two-port coupled inductor is presented as an example.**

***Index Terms*— transient circuit simulation, Foster's canonical model.**

I. Introduction

Transient simulation of circuits incorporating distributed structures has been particularly troublesome. Electromagnetic characterization of transmission lines, antennas and RF and microwave structures, especially when the impact of skin effect and related frequency-dependent ohmic loss must be taken into account, can only be determined accurately in the frequency domain using one of several integral equation-based or differential equation-based electromagnetic field solvers. Subsequently, for the purposes of (in general) nonlinear transient simulation of RF subsystems and systems, a transformation technique is required to obtain time-domain transfer functions for such passive components from their frequency-domain responses. Particular issues include convergence problems, non-causality inherent in the time-domain transformation, aliasing problems in the conversion, lengthy convolution and nonlinear iterations, and numerical ill-conditioning. Furthermore, even small numerical errors in the frequency-domain characterization may manifest themselves as appreciable waveform errors in the transient response. The same is true in reverse, potentially rendering transient simulation inadequate for the design of strongly frequency-dependent microwave circuits such as circuits with filters and matching networks.

Transient analysis is critical when analyzing large RF circuits with important transient behavior, especially when large-signal non-linear responses must be predicted, when thermal effects on device behavior must be taken into account, or when avalanche occurs. Such simulations are critical for predicting and mitigating oscillation and chaotic behavior. Clearly, in order to ensure the integrity and accuracy of such simulations, the calculated responses must be free from spurious non-physical

This material is based upon work supported in part by the Space and Naval Warfare Systems Center San Diego under grant number N66001-01-1-8921 through North Carolina State University as part of the DARPA NeoCAD Program.

R. Mohan, S. E. Mick, F. P. Hart, K. Chandrasekar, P. D. Franzon, M. B. Steer are with the Department of Electrical and Computer Engineering, North Carolina State University, Raleigh, NC 27695-7911. M. J. Choi and A. C. Cangellaris are with the University of Illinois Urbana Champaign, Urbana-Champaign, Illinois.

oscillations and instabilities caused by lack of stability or passivity of the numerically generated frequency-domain multipart descriptions of the passive components. The purpose of this transaction is to introduce a Foster-synthesis based methodology for the development of a passive reduced-order multiport description of such passives from numerically calculated frequency-domain data, and discuss its implementation in the transient circuit simulator fREEDA®.

II. Background

Many techniques have been explored for incorporating distributed structure frequency-domain characterizations in transient circuit simulators. These have been extensively reviewed recently by Achar *et al.* [1]. Techniques include developing the impulse response and then using convolution-based iteration techniques [2], [3] and also more recently the evaluation of convolutions in a recursive manner [4]. Asymptotic Waveform Evaluation (AWE) [5] and Laplace Inversion [6] are powerful, but have their limitations in application as described in the following paragraphs.

A. Asymptotic Waveform Evaluation

The AWE method is best suited for use in conjunction with characterizations for which the moments of the transfer function are either readily available or can be computed with high accuracy. The basic objective of AWE is to develop a reduced-order state-space model of a linear sub-component of a system for the purposes of expediting transient simulation. According to [5], application of AWE results in about 2 orders of magnitude reduction in the simulation time needed if the original system (of higher order) is used. To facilitate the utilization of AWE in nonlinear circuit simulation numerical inversion, convolution and piecewise linearization methods have been introduced [5], [7]. The original implementation of the AWE technique was found to be of low bandwidth, a consequence of the fact that moment matching was based on a single-point Padé approximation. This limitation was partially addressed through the use of multipoint Padé approximations (e.g.,[8]). More recently, more systematic methodologies have been proposed for such Padé approximation-based model order reduction which, through special processes, can ensure the passivity and, hence, stability, of the generated reduced-order model (see, for example, [9], [10]). However, use of such model order reduction methods assumes that the mathematical statement of the discrete electromagnetic boundary value problem used to characterize the passive structure is in a form compatible with the Krylov-subspace formalism that constitutes the backbone of all such methods. While finite difference- and finite element-based methods produce such models [11], this is not the case of integral equation-based solvers in general, unless quasi-static approximations of the full-wave Green's function kernels involved in the integral statements are made (e.g., [12]).

Nevertheless, with the advent of fast and numerically-stable iterative methods for the iterative solution of full-wave integral equations, their application to the full-wave characterization of distributed passive components and interconnects continues to grow. Since AWE-like and Krylov subspace techniques are not best suited for the development of reduced-order models from the method-of-moments approximations of these full-wave integral equations, one has to rely on other means for the synthesis of multiport models from the calculated frequency domain responses sampled at multiple frequency points over the desired frequency bandwidth. The convolution-based development of the impulse response discussed next is one of these techniques.

B. Convolution Based on Impulse Response

This technique suffers from two major limitations. One of these is the aliasing problem associated with the inverse Fourier transform operation required to extract the impulse response from frequency-domain characteristics. Many schemes have been developed for extending the dynamic range but have proved difficult to apply in general. Causality has been a long-running problem but has been alleviated recently [2]. Even if the aliasing problem is avoided, the convolution approach suffers from excessive run times. The convolution integral, which becomes a convolution sum in computer simulations, is O(N_T^2) when it is implemented (N_T being the total number of discrete time points used to divide the continuous time) [3].

C. Numerical Inversion of Laplace Transform Technique

This technique does not have aliasing problems since it does not assume that the function is periodic – the inverse transform exists for both periodic and non-periodic functions. There is no causality problem for double-sided Laplace transforms, either. Unlike FFT-based methods, the desired part of the response can be obtained without performing tedious and unnecessary calculations for the other parts of the response. However Laplace techniques suffer from the limitations of series approximations and the nonlinear iterations involved. The advantages and limitations of the inverse Laplace methods are discussed in detail in [6], [13].

D. Summary

Irrespective of the method used for the development of a circuit simulator-compatible impulse response, a process that ensures the passivity (or at least the stability) of the synthesized response is required. Passivity is an issue that continues to receive significant attention by the electronic CAD community as subsystem- and system-level nonlinear, transient simulation of complex circuits involving sections that exhibit distributed electromagnetic behavior becomes indispensable for design optimization and functionality verification [14],[15]. The Foster's synthesis-based technique which we will discuss next includes such a process. However, prior to its discussion the important issue of the assignment of *local references* for different ports in the distributed system is briefly reviewed.

III. Local Reference Groups

Most microwave networks can be viewed as inter connections of N-port networks, where each port has two terminals one of which is a reference terminal. In the case of a distributed network these reference terminals are, in general, independent of each other. In many cases the appropriate handling of the reference terminals is inherent in the network parameters used, such as with the use of S-parameters. Use of multiple reference terminals is of paramount importance to the proper electromagnetic description of large distributed networks such as active antenna arrays and on-chip interconnect networks [16], [17]. The formulation particular suited to circuit analysis is the Local Reference Group (LRG) concept [16], [18]. The difference between LRGs and the conventional usage of ports will now be explained. Conventionally, when referring to an N-port we are referring to a network with N nonreference terminals and N reference terminals. (The reference terminals are not instantaneously connected and so it is an error to consider them as a global ground node.) In the general case, several terminals can have the same Local Reference Terminal (LRT) and the network parameters describing the subcircuits are port-based. The conversion of the port-based Y parameters to nodal-based Y parameters, as are required in nodal-based circuit simulators, has been previously defined by us [19]. In effect an LRG is a multiterminal port with one reference terminal and one or more other terminals.

IV. Foster's Canonical Model

Foster's canonical model is used by us to develop a reduced-order model of a distributed network [24]. Of most importance here is that, when properly constructed, Foster's canonical model is causal.

A. Representation

Foster's representation of distributed circuits is adopted because of its guaranteed causality, provided that its construction from the available frequency-domain data for the network response is carried out according to the constraints involved in its definition. The detail description of these constraints, along with a description of the methodology used for the synthesis of Foster's canonical form, can be found in [23]. It is pointed out that, for our purposes, the methodology proposed in [23] was streamlined for direct compatibility with the rational function synthesis algorithm VectFit [21], [22]. The resulting process was first presented in [25]. It is important to stress that prior to utilizing VectFit, the numerical data for the frequency-domain response, which constitute the input to VectFit, are tested for passivity. Violation of passivity may be encountered, particularly in relation to data obtained from numerical solutions, in which case it is predominantly caused by discretization or round-off error. The easiest way to test for passivity is through the conditions satisfied by the scattering-parameters of the multiport circuit [20]. If passivity is violated at a frequency point, the situation is rectified through a slight perturbation of the scattering parameters.

Once the numerical data has been rendered passive, the Foster synthesis process is ready to commence. To offer a brief review of the properties of the Foster canonical form, the case of a one-port circuit is considered. Foster's canonical representation of its input admittance is,

$$\begin{aligned} H(s) = \quad & H_0 + H_1 s \\ & + \sum_{k=1}^{m} \left(\frac{r_k}{s-p_k} \right) + \sum_{k=1}^{m} \left(\frac{a_k}{s-b_k} + \frac{\overline{a}_k}{s-\overline{b}_k} \right) \end{aligned} \quad (1)$$

where H_0 represents the conductance term, H_1 represents the capacitance value of the shunt capacitance term, $r_k/(s-p_k)$ represents a real pole at $s = b_k$, and $a_k/(s-b_k)$ and $\overline{a}_k/(s-\overline{b}_k)$ — the overbar indicates the complex conjugation — together represent a complex conjugate pole pair. In addition to the requirement that the real part of the poles is non-positive, the requirement that H_0 and H_1 are non-negative is recognized immediately and intuitively as a required constraint for passivity. These constraints are complemented by ones involving the coefficients r_k, and a_k and the associated poles. These additional constraints are

$$\Re r_k \geq 0, \quad \Re a_k > 0, \quad 0 \leq \Im a_k \Im b_k \leq \Re a_k \Re b_k \quad (2)$$

The constraints for the case of multiport network are of similar form and can be found in [23]. A final point worth mentioning is the issue of the accuracy of the synthesized model outside the frequency range of the data used for its synthesis. Clearly, accuracy is guaranteed only over the frequency range used in the synthesis. It is, therefore, essential that the frequency range over which data is generated for the synthesis of the Foster equivalent circuit is selected broad enough to encompass the anticipated bandwidth of interest in the simulations of the circuits in which the synthesized equivalent will be used.

Synthesized subject to these constraints, the multiport admittance matrix is guaranteed to be passive and hence, causal. Its compatibility with the Modified Nodal Admittance (MNA) matrix description of the state-space representation of the overall system is another advantage that becomes more evident from the discussion in the following section.

Returning to the general case of a multiport distributed circuit, let N be the number of ports. The pole-residue form of its rational function approximation, obtained according to the process outlined above, is as follows

$$\mathbf{Y}(s) = \begin{bmatrix} \sum_{k=1}^{M} \frac{r_k^{11}}{s-p_k} & \cdots & \sum_{k=1}^{M} \frac{r_k^{1N}}{s-p_k} \\ \vdots & \sum_{k=1}^{M} \frac{r_k^{ij}}{s-p_k} & \vdots \\ \sum_{k=1}^{M} \frac{r_k^{N1}}{s-p_k} & \cdots & \sum_{k=1}^{M} \frac{r_k^{NN}}{s-p_k} \end{bmatrix}$$

$$= \begin{bmatrix} y_{11}(s) & \cdots & y_{N1}(s) \\ \vdots & y_{ij}(s) & \vdots \\ y_{1N}(s) & \cdots & y_{NN}(s) \end{bmatrix} \quad (3)$$

where all the elements share the same set of *M* poles: p_1, p_2, ... , p_M. The poles are, in general, complex and, due to the passivity of the generated reduced model, are all stable. Since complex poles occur in complex conjugate pairs, with their corresponding residues being complex conjugates also, the expression for the current at the j th port in terms of the *N*-port voltages may be cast in the form:

$$i_i = \begin{bmatrix} \sum_{k=1}^{M_R} \frac{R_{rk}^{1j}}{s-P_{rk}} \\ + \sum_{k=1}^{M_C} \frac{\left(R_{ck}^{1j}+\bar{R}_{ck}^{1j}\right)s-\left(R_{ck}^{1j}\bar{P}_{ck}+\bar{R}_{ck}^{1j}P_{ck}\right)}{s^2-\left(P_{ck}+\bar{P}_{ck}\right)s+|P_{ck}|^2} \end{bmatrix} v_1 + \cdots$$
$$\begin{bmatrix} \sum_{k=1}^{M_R} \frac{R_{rk}^{ij}}{s-P_{rk}} \\ + \sum_{k=1}^{M_C} \frac{\left(R_{ck}^{ij}+\bar{R}_{ck}^{ij}\right)s-\left(R_{ck}^{ij}\bar{P}_{ck}+\bar{R}_{ck}^{ij}P_{ck}\right)}{s^2-\left(P_{ck}+\bar{P}_{ck}\right)s+|P_{ck}|^2} \end{bmatrix} v_j + \cdots$$
$$\begin{bmatrix} \sum_{k=1}^{M_R} \frac{R_{rk}^{Nj}}{s-P_{rk}} \\ + \sum_{k=1}^{M_C} \frac{\left(R_{ck}^{Nj}+\bar{R}_{ck}^{Nj}\right)s-\left(R_{ck}^{Nj}\bar{P}_{ck}+\bar{R}_{ck}^{Nj}P_{ck}\right)}{s^2-\left(P_{ck}+\bar{P}_{ck}\right)s+|P_{ck}|^2} \end{bmatrix} v_N \quad (4)$$

where M_C is the number of pairs of complex poles and M_R is the number of real poles. Thus (4) describes one row of the definite port-based nodal admittance matrix: i_i = $y_{1j}v_1$ + ... + $y_{ij}v_j$ + ... + $y_{Nj}v_N$. This is derived from the indefinite form of the nodal admittance matrix with multiple redundant rows and each of these corresponding to an LRT [16], [24]. In the case of a lumped linear network with a single global reference terminal, there would be only one redundant row. This distinction is not important for the development that follows but is critical in formulating the circuit equations for the entire network. Thus, referring to the LRG section, each of the LRTs shown (terminals E_1,...,E_m,...,E_M) result in redundant entries and care must be taken in formulating the overall circuit equations. In the end the definite forms of the total MNA matrix must be used as the indefinite form is singular [19]. The synthesis methodology is then based on the interpretation of each of the terms in the equation above as part of an equivalent circuit.

B. Technical Approach

The N-port Foster's model is directly incorporated in the Modified Nodal Admittance (MNA) matrix in the circuit simulator. The implementation is analogous to that of inserting multi-terminal linear Voltage Controlled

Current Sources (VCCSs) although a direct implementation is preferred for simulation speed and robustness as well as netlist robustness (that is specifying a single element rather than a complex circuit of VCCSs). The method demonstrated here is the *Pole-Residual* method as it has demonstrated good numerical stability.

Foster's model describes an admittance matrix wherein each element of the matrix is represented as a rational function in pole-residue format. In this format different elements in the admittance matrix may have different poles (meaning values of the poles). But all the elements in the admittance matrix must have the same number of poles. However in a complete network simulation there can be any number of N-port Foster models with each model having a different number of poles. The restriction on the number of poles of each of the admittance matrix elements being the same comes about because time-domain analysis requires derivatives of the modified nodal admittance matrix. (For steady-state analysis, as in Harmonic Balance analysis, there would not be this pole restriction but the key guiding principal we have followed is using the same model in all circuit analyses.)

C. Filling the MNA Matrix

The widely accepted practice for incorporating models in a simulator is to use a stamp which in this case is a submatrix entry in the MNA matrix of the linear network. This is done using a function typically called `fillMNAM` which in our case fills the MNA matrix with the calculated transfer function values.

Consider a 2-port distributed network, then we could have either 1 or 4 instances of the NPortFoster element. That is, if

$$\mathbf{Y}(s) = \begin{bmatrix} H_{11}(s) & H_{12}(s) \\ H_{21}(s) & H_{22}(s) \end{bmatrix} \tag{5}$$

then each $H_{ij}(s)$ could be represented as an instance of this element, depending on the way it is connected in the network. Alternatively all four components of the matrix could be treated as a single element. However simplicity is critically important and so each element of the admittance matrix is implemented separately. Furthermore, each admittance element has one or more real poles and one or more complex pole pairs. From (3),

$$y_{ij} = \sum_{k=1}^{m} y_{ijk} \tag{6}$$

where

$$y_{ijk} = \frac{R_{rk}^{ij}}{s - P_{rk}} + \frac{\left(R_{ck}^{ij} + \bar{R}_{ck}^{ij}\right) s - \left(R_{ck}^{ij}\bar{P}_{ck} + \bar{R}_{ck}^{ij} P_{ck}\right)}{s^2 - \left(P_{ck} + \bar{P}_{ck}\right) s + |P_{ck}|^2}. \tag{7}$$

Thus (6) can be written in the form:

$$y_{ijk} = \left(\frac{r_{ijk}}{s - p_{ijk}}\right) + \left(\frac{A_{ijk}s + B_{ijk}}{s^2 + C_{ijk}s + D_{ijk}}\right). \tag{8}$$

Hence there is a real pole-residue value and a complex pole-residue value and the complex pole-residue value is converted to real pole-residue format.

D. Development of the MNA Stamp

In this section the MNA stamp of Foster's model is developed. The transfer function $H(s)$, Voltage $V(s)$ and the Current $I(s)$ are related as:

$$I(s) = H(s)V(s) \tag{9}$$

and

$$H_{ijk}(s) = \left(\frac{r_{ijk}}{s - p_{ijk}}\right) + \left(\frac{a_{ijk}}{s - b_{ijk}} + \frac{\overline{a}_{ijk}}{s - \overline{b}_{ijk}}\right) \tag{10}$$

where k varies from 1 to M. The MNA stamp is built from stamps for the individual poles. First consider the real pole,

$$\left(\frac{r_{ijk}}{s - p_{ijk}}\right) \tag{11}$$

then

$$I_i(s) = \left(\frac{r_{ijk}}{s - p_{ijk}}\right) V_j(s) \tag{12}$$

taking its inverse Laplace transform and rearranging,

$$i_i + \left(\frac{r_{ijk}}{p_{ijk}}\right) v_j - \left(\frac{1}{p_{ijk}}\right) \frac{di_i}{dt} = 0 \tag{13}$$

where $v = v_m - v_n$ is the voltage difference between terminals m and n. The real pole adds one extra row and column. Then the MNA matrix stamp for y_{ijk} is, in conventional form [26],

$$\begin{array}{c} \\ \\ m \\ n \\ m+1 \end{array} \quad \begin{array}{c} \begin{array}{ccc} v_m & v_n & i_i \\ & & m+1 \end{array} \\ \left[\begin{array}{cc|c} & & 1 \\ & & -1 \\ \hline r_{ijk} & -r_{ijk} & p_{ijk} \end{array}\right] \end{array} \tag{14}$$

and its first derivative is

$$\begin{array}{c} \frac{di_i}{dt} \\ \left[\begin{array}{c|c} & \\ & \\ \hline & -1 \end{array}\right] \end{array}. \tag{15}$$

Next consider the complex conjugate pole pair,

$$\left(\frac{a_{ijk}}{s - b_{ijk}}\right) + \left(\frac{\overline{a}_{ijk}}{s - \overline{b}_{ijk}}\right) \tag{16}$$

when multiplied it yields the real term,

$$\left(\frac{A_{ijk}s + B_{ijk}}{s^2 + C_{ijk}s + D_{ijk}}\right) \tag{17}$$

and so

$$I_i(s) = \left(\frac{A_{ijk}s + B_{ijk}}{s^2 + C_{ijk}s + D_{ijk}}\right) V_j(s) \tag{18}$$

where A_{ijk}, B_{ijk}, C_{ijk} and D_{ijk} are real and

$$A_{ijk} = 2a_{ijk} \tag{19}$$

$$B_{ijk} = 2a_{ijk}c_{ijk} - 2b_{ijk}d_{ijk} \tag{20}$$

$$C_{ijk} = -2c_{ijk} \tag{21}$$

$$D_{ijk} = c_{ijk}^2 + d_{ijk}^2 \tag{22}$$

Taking the inverse Laplace transform of (18) and rearranging,

$$\frac{d^2 i_i}{dt^2} + C_{ijk}\frac{di_i}{dt} + D_{ijk}i_i - A_{ijk}\frac{dv_j}{dt} - B_{ijk}v_j = 0 \tag{23}$$

Since this involves second derivative terms, we take an auxiliary variable, say x, and define it as:

$$x = \frac{di_i}{dt} \tag{24}$$

and so

$$\frac{dx}{dt} = \frac{d^2 i_i}{dt^2} \tag{25}$$

then the MNA stamp is

$$\begin{array}{c} \\ m \\ n \\ i_i \\ x \end{array} \quad \begin{array}{c} \begin{array}{cccc} v_m & v_n & i_i & x \end{array} \\ \left[\begin{array}{cc||c|c} & & 1 & \\ & & -1 & \\ \hline\hline -B_{ijk} & B_{ijk} & D_{ijk} & \\ \hline & & 1 & \end{array}\right] \end{array} \tag{26}$$

and its first derivative is

$$\begin{array}{c} \\ m \\ n \\ i_i \\ \frac{dx}{dt} \end{array} \quad \begin{array}{c} \begin{array}{cccc} v_m & v_n & i_i & \frac{dx}{dt} \end{array} \\ \left[\begin{array}{cc||c|c} & & & \\ & & & \\ \hline\hline -A_{ijk} & A_{ijk} & C_{ijk} & 1 \\ \hline & & & 1 \end{array}\right] \end{array}. \tag{27}$$

The number of extra rows and columns of the MNA for the implementation of time domain analysis is,

$$\begin{aligned} \text{Extra rows and columns} = {} & \text{number of real pole} \\ & + 2 \times \text{number of complex pole} \end{aligned}$$

The factor of two is present here because of the complex conjugate pairs.

V. Modeling of a Distributed Coupled Inductor

Coupled inductors or on-chip transformers are used in radio frequency and microwave integrated circuits to boost inductance values, as balun-like structures, as AC coupled interconnects and in switched capacitor bias circuits operating at microwave frequencies. A Stacked transformer of external dimension of 50 μm and 75 μm was fabricated on a 0.25 μm, five metal layer process [27], see Fig. 1. The self-inductances of the transformer are nominally 2 nH. A patterned polysilicon ground shield was placed between the bottom spiral inductor and the substrate to reduce eddy currents and eliminate substrate effects.

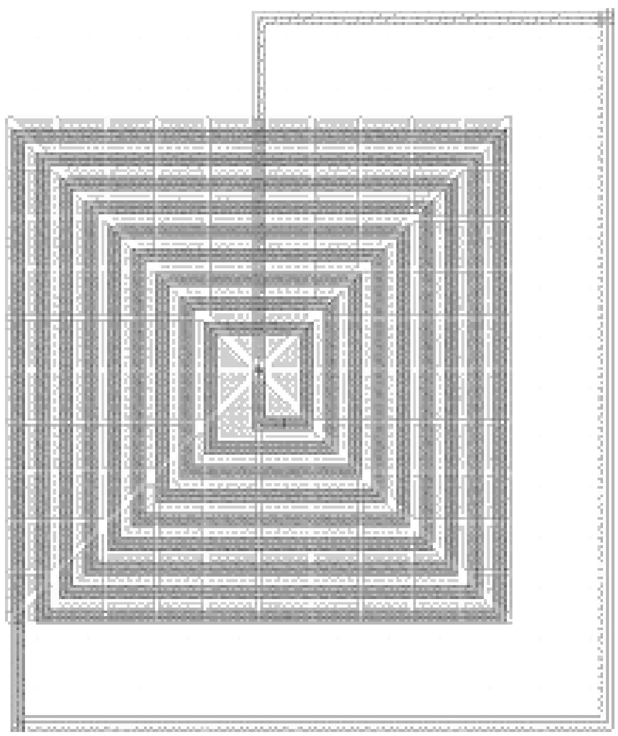

Fig. 1. 3D picture of on-chip coupled inductors.

The distributed coupled inductor, Fig. 1, has complex frequency characteristics, Fig. 2, and demonstrates the fidelity of the reduced-order model and its integration in a transient circuit simulator. An N th order port-based Y-parameter Foster's canonical model was developed from the swept frequency experimental network analyzer characterization. Note that the Foster's model is guaranteed to be causal and hence no check is required.

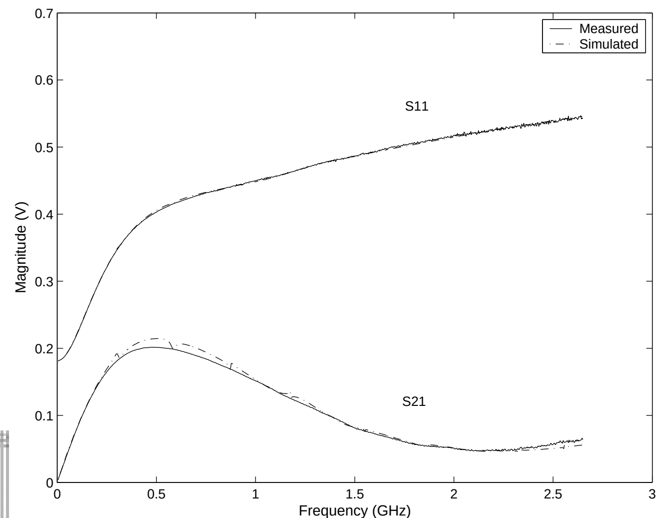

Fig. 2. S parameters of the coupled inductor.

A. Experimental Setup

The experimental setup consists of a probe station, digital sampling oscilloscope, 3 Gbps pulse generator, SMA cables and 100 μm pitch Ground-Signal-Ground (GSG) probes.

The system was initially calibrated by applying a square pulse of 1 GHz frequency using an SMA cable and the GSG probes. The output port was connected to the sampling head of the oscilloscope using GSG probes an SMA cable.

The input signal frequency of 1 GHz is low enough that it is unaffected by discontinuities and dispersive losses in the SMA cable. To that end the GSG probes were connected in a through configuration on a LRM ISS calibration substrate and the output waveform on the oscilloscope was analyzed. It was observed that the difference in the two waveforms (both in amplitude and frequency) was negligible. Hence this confirms that the effect of losses in the SMA cable or discontinuity effect in the fixturing is not significant enough to warrant a time domain calibration. This is illustrated in Fig. 3 where two wave forms are compared: one measured at the output of the pulse generator and the other at the end of a through line connection.

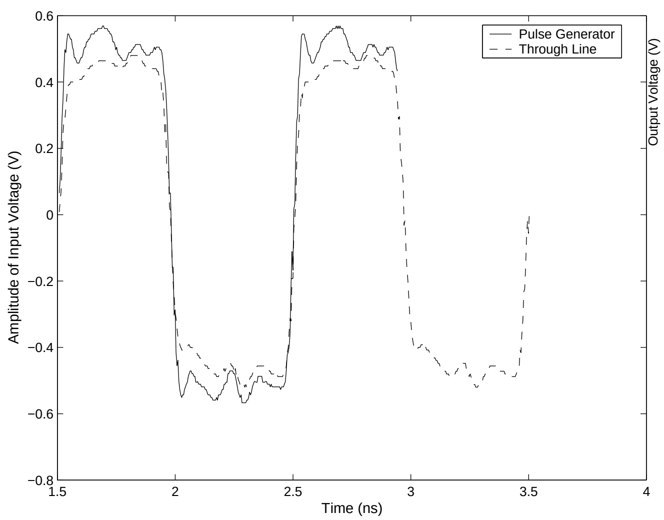

Fig. 3. Comparison of the pulse waveforms measured at the output of the pulse generator and at the end of the through line.

B. Results and Discussion

Fig. 4 shows the transient response of the coupled inductor calculated using the NPortFoster model described above. N was taken to be 2, as it is a two-port inductor model and the factorization time of the matrix was calculated to be 0.01 seconds. The drive for the 2-port Foster's network is a 1 V exponential square input pulse with a series resistor of 50-Ohm. The output voltage is measured across a 50-Ohm resistive load and the transient analysis simulation is shown in Fig. 4. The simulation result agree closely with that of the experimental data. In particular, the direct implementation described minimizes the number of nonlinear operations where as a large number of such operations are required if a synthesized RLCK (K being a coupled inductor) equivalent circuit was used.

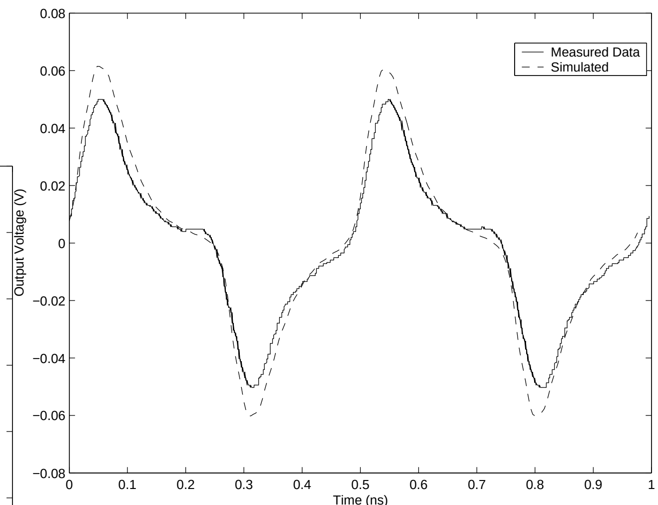

Fig. 4. Complete transient response for the coupled inductor comparing measured and simulated results.

VI. Conclusion

This paper has presented the result of a quest for a distributed structure modeling technology that can be used in transient circuit simulation analysis strategy. The modeling technique has guaranteed causality and is particularly well suited to modeling distributed structures that do not necessarily have low pass characteristics. The modeling technique can be efficiently implemented in a transient circuit simulator (in this case fREEDA® [28]).

VII. Acknowledgement

The authors would like to thank J. Nath, Department of Electrical and Computer Engineering, North Carolina State University for useful suggestions in the experimental setup of the coupled inductor.

REFERENCES

[1] R. Achar and M. S. Nakhla, “Simulation of High Speed Interconnects,” *Proc. of the IEEE*, Vol. 89, no.5, May 2001, pp. 693–728.

[2] T. J. Brazil, “A new method for the transient simulation of causal linear systems described in the frequency domain,” in *1992 IEEE MTT-S Int. Microwave Symp. Dig.*, Vol. 3, June 1992, pp. 1485–1488.

[3] M. S. Basel, M. B. Steer and P. D. Franzon, “Simulation of high speed interconnects using a convolution-based hierarchical packaging simulator,” *IEEE Trans. Advanced Packaging*, Vol. 18, Feb. 1995, pp. 74–82.

[4] M. Celik, L. Pileggi and A. Odabasioglu, *IC Interconnect Analysis*, Reading, Kluwer Academic Publishers, 2002.

[5] R. J. Trithy and R. A. Rohrer. “AWE macromodels for nonlinear circuits,” *Proc. 36 th Midwest Symp. Circuits Systems*, Vol. 1, Aug. 1993, pp. 633–636.

[6] L. Brancik, “An improvement of FFT-based numerical inversion of two-dimensional Laplace transforms by means of epsiv-algorithm,” *IEEE Int. Symp. on Circuits and Systems*, Vol. 4, May 2000, pp. 28–31.

[7] E. Chiprout and M. Nakhla. “Fast nonlinear waveform estimation for large disributed networks,” in *1992 IEEE MTT-S Int. Microwave Symp. Dig.*, June 1992, pp. 1341–1344.

[8] M. Celik, O. Ocali, M. A. Tan and A. Atalar, “Pole-zero computation in microwave circuits using multipoint Padè approximation,” *IEEE Trans. Circuits and Systems*, Vol.14, Jan. 1995, pp. 6–13.

[9] A. Odabasioglu, M. Celik, and L.T. Pileggi, “PRIMA: Passive reduced-order interconnect macromodeling algorithm,” *IEEE Trans. Computer-Aided Design of Integrated Circuits and Systems*, Vol. 17, no. 8, Aug. 1998, pp. 645–654.

[10] R. W. Freund, “Passive reduced-order modeling via Krylov-subspace methods,” *IEEE Int. Symp. Computer-Aided Control System Design, CACSD 2000*, Sep. 2000, pp. 261–266.

[11] Y. Zhu and A. C. Cangellaris, “A new finite element model for reduced order electromagnetic modeling,” *IEEE Microwave and Wireless Components Lett.*, Vol. 11, no. 5, May 2001, pp. 211–213.

[12] M. Kamon, N. A. Marques, L. M. Silveira and J. White, “Automatic generation of accurate circuit models of 3-D interconnect,” *IEEE Trans. Comp. Pack. and Manufacturing Tech. - Part B*, Vol. 21, no. 3, Aug. 1998, pp. 225–234.

[13] A. Yonemoto, T. Hisakado and K. Okumura, “An improvement of convergence of FFT-based numerical inversion of Laplace transforms,” *IEEE Int. Symp. on Circuits and Systems*, Vol. 5, May 2002, pp.26–29.

[14] H. Chen and J. Fang, ”Enforcing bounded realness of s parmeter through trace parameterization,” *Proc. 2003 IEEE Topical Meeting on Electrical Performance of Electronic Packaging*, Oct. 2003, pp. 291 – 294.

[15] D. Saraswat, R. Achar, and M. Nakhla, ”Enforcing passivity for rational function based macromodels of tabulated data,” *Proc. 2003 IEEE Topical Meeting on Electrical Performance of Electronic Packaging*, Oct. 2003, pp. 295 – 298.

[16] A. I. Khalil and M. B. Steer, “Circuit theory for spatially distributed microwave circuits,” *IEEE Trans. on Microwave Theory and Tech.*, Vol. 46, Oct. 1998, pp. 1500-1503.

[17] J. Kunisch and I. Wolff, “The compression approach: A new technique for the analysis of distributed circuits containing nonlinear elements,” in *1992 IEEE MTT-S Int. Microwave Symp. Workshop WSK*, pp. 16-31, 1992.

[18] C. E. Christoffersen and M. B. Steer, “Implementation of the local reference node concept for spatially distributed circuits,” *Int. J. RF and Microwave Computer Aided Engin.*, Vol. 9, Sept. 1999, pp. 376–384.

[19] R. Mohan, *Integration of Interconnect Models in a Transient Circuit Simulator*, M. S. Thesis, Dept. of Electrical and Computer Engineering, North Carolina State University, 2003.

[20] D. Pozar, *Microwave Engineering*, Reading, Massachusetts, 1993.

[21] B. Gustavsen and A. Semlyen, “Rational approximation of frequency-domain responses by vector fitting,” *IEEE Trans. Power Delivery*, Vol. 14, Jul. 1999, pp. 1052–1061.

[22] B. Gustavsen, ”Computer code for rational approximation of frequency dependent admittance matrices,” *IEEE Trans. Power Delivery*, Vol. 17, Oct. 2002, pp. 1093–1098.

[23] T. Mangold and P. Russer, “Full-wave modeling and automatic equivalent-circuit generation of millimeter-wave planar and multiplayer structures,” *IEEE Trans. Microwave Theory and Tech.*, Vol. 47, no. 6, Jun. 1999, pp. 851–858.

[24] M. J. Choi, K. P. Hwang and A. C. Cangellaris, “Direct generation of SPICE-compatible passive reduced-order models of ground/power planes,” in *Proc. 50th Electron. Comp. Technol. Conf.*, May 2000, pp. 775–780.

[25] M. J. Choi and A. C. Cangellaris, “A quasi three-dimensional distributed electromagnetic model for complex power distribution networks,” *IEEE Trans. on Advanced Packaging*, Vol. 25, Feb. 2002, pp. 28–34.

[26] J. Vlach and K. Singhal, *Computer Methods for Circuit Analysis and Design*, Reading, Van Nostrand Reinhold, 1994.

[27] S. Mick, J. Wilson and P. D. Franzon, “4 Gbps high-density AC coupled interconnection,” *IEEE Custom Integrated Circuits Conf.*, May 2002, pp. 133–140.

[28] W. Batty, C. E. Christoffersen, A. B. Yakovlev, J. F. Whitaker, M. Ozkar, S. Ortiz, A. Mortazawi, R. Reano, K. Yang, L. P. B.

Katehi, C. M. Snowden and M. B. Steer, “Global coupled EM-electrical-thermal simulation and experimental validation for a spatial power combining MMIC array,” *IEEE Trans. Microwave Theory and Tech.*, Vol. 50, Dec 2002, pp. 2820–2833.